N91-21209

CRITICAL SPEEDS and FORCED RESPONSE SOLUTIONS or ACTIVE MAGNETIC BEARING TURBOMACHINERY, Part I

J. Keesee, D. Rawal, R. Gordon Kirk
Virginia Polytechnic Institute and State University
Department of Mechanical Engineering
Randolph Hall
Blacksburg
VA 24061-0238

CRITICAL SPEEDS AND FORCED RESPONSE SOLUTIONS FOR ACTIVE ACTIVE MAGNETIC BEARING TURBOMACHINERY PART I

J. Keesee, Research Assistant
D. Rawal, Research Assistant
R. G. Kirk, Associate Professor

Virginia Polytechnic Institute and State University
Blacksburg, VA

ABSTRACT

The prediction of critical speeds and forced response of active magnetic bearing turbomachinery is of great interest due to the increased use of this new and promising technology. Calculating the system undamped critical speeds and forced response is important to all those who are involved in the design of the active magnetic bearing system. This paper is the first part of a two part paper which presents the theory and results of an investigation into the influence of sensor location on the undamped critical speeds and forced response of the rotor and bearing system.

Part I of this paper concentrates on an extended Jeffcott model which was used as an approximate solution to a more accurate transfer matrix procedure. Theory behind a two-degree-of-freedom extended Jeffcott model will be presented. Results of the natural frequency calculation will be shown followed by the results of the forced response calculation. The system response was predicted for two types of forcing. A constant magnitude excitation with a wide frequency variation was applied at the bearings as one forcing function. The normal unbalance force at midspan was the second source of excitation. The results of this extended Jeffcott solution gives useful design guidance for the influence of the first and third modes of a symmetric rotor system.

NOMENCLATURE

A shaft relative motion max amplitude for 1st mode (cm)

a mass eccentricity of imbalance (cm)

B shaft relative motion max amplitude for 3rd mode (cm)

C ratio of bearing damping to shaft damping (dim)

C_1 damping of AMB (N-s/cm)

C_2 damping of flexible shaft (N-s/cm)

$F\phi$ constant magnitude force applied to journal mass (N)

i square root of -1, complex variable (dim)

K ratio of bearing stiffness to shaft stiffness (dim)

K_1 stiffness of AMB (N/cm)

K_2 stiffness of flexible shaft (N/cm)

K_{11} row 1, column 1 of stiffness matrix in Jeffcott solution

K_{12} row 1, column 2 of stiffness matrix in Jeffcott solution

K_{21} row 2, column 1 of stiffness matrix in Jeffcott solution

K_{22} row 2, column 2 of stiffness matrix in Jeffcott solution

L bearing span (cm)

M ratio of bearing journal mass to rotor midspan mass (dim)

M_1 equivalent bearing journal mass (kg)

M_2 equivalent rotor midspan mass (kg)

R shaft absolute displacement (cm)

X shaft maximum displacement in the X-direction (cm)

r_1 shaft deflection at bearing journal location (cm)

r_2 shaft deflection at midspan mass (cm)

r_s shaft deflection at AMB sensor location (cm)

z axial distance along rotor (cm)

z_s axial distance to AMB sensor (cm)

α sensor relative position to midspan (dim)

β normalized shaft motion at sensor location (dim)

ω angular velocity of shaft (rad/s)

Ω natural frequency normalized to rigid bearing critical speed (dim)

INTRODUCTION

The evaluation of critical speeds and forced response for turbomachinery with fluid-film and antifriction bearings is now standard design practice for many manufacturers. The standard transfer matrix solution technique (Myklestad, 1944; Prohl, 1945) is the current industry standard for evaluation of rotor response and undamped critical speeds. More recently interest in improved forced response and stability of high pressure compressors and pumps have forced designers to consider active magnetic bearings (AMBs) for either retrofit or new machinery application. The initial application of magnetic bearings to centrifugal compressor was evaluated using standard critical speed codes without consideration for sensor location (Hustak et al., 1987; Schoeneck and Hustak, 1987). The comparisons of predicted response and critical speed placement to actual test and field results (Hustak et al., 1987; Schoeneck and Hustak, 1987; Kirk et al., 1988) have drawn attention to possible improvements in the analytical representation of the magnetic bearings.

This paper is the first of a two part paper which presents an evaluation of the effect of sensor location on the predicted undamped critical speeds and forced response of turbomachinery. This paper concentrates on the solution of a two-degree-of-freedom model developed by extending the original Jeffcott model to include bearing stiffness and damping, journal mass and accounting for non-colocation of bearing and sensor. The second paper will discuss the evaluation of a modified transfer matrix solution and will present results of a typical rotor bearing system analysis.

The extended Jeffcott model will be considered to have sensors either inboard or outboard of the bearing centerline. The system response is calculated for two different types of forcing functions. The first excitation force is the usual unbalance located at the midspan mass. The second is a constant magnitude excitation applied at the journal mass while the excitation frequency is varied. The second type of rotor excitation is available in an actual active magnetic bearing and rotor system.

PRINCIPLE OF ACTIVE MAGNETIC BEARING OPERATION

The AMB is composed of two major mechanical parts, the rotor and the stator. Both are made of ferromagnetic laminations. The rotor laminations are placed on the machine shaft at the selected journal location. The stator laminations are slotted and include windings to provide the magnetic levitation and position control. For each degree of freedom, two electromagnets are required since they operate by attraction only. Figure 1 shows the stator

lamination construction of a radial bearing and sensor with the rotor lamination sleeve in the background.

Rotor position is monitored by sensors and this signal is compared to a nominal reference signal with a closed loop controller which supplies a command signal to the power amplifiers. These amplifiers provide power to the electromagnets to resist rotor movement from the nominal position. The design of the control loop gives the option to select the effective bearing stiffness and damping. The details of this design procedure are not the subject of this paper but the values of stiffness and damping must be carefully selected to give the rotor system the desired optimum dynamic response and stability.

Before power is applied to the bearings, the rotor is supported on two auxiliary ball bearings located in close proximity to the AMB. The clearance between the rotor and the inner race of the ball bearing is selected to prevent rotor contact with the AMB pole pieces or the internal seals of the compressor while the rotor is at rest or during an emergency shutdown. When power is applied to the electronic controls, the electromagnets levitate the rotor in the magnetic field and rotation by the driving source, such as a motor or turbine, can be started. The sensors and control system regulate the strength and direction of the magnetic fields to maintain exact rotor position by continually adjusting to the changing forces on the rotor. Should both the main and redundant features of the AMB fail simultaneously, the auxiliary bearing and rotor system are designed to permit safe deceleration.

When the turbomachine is running the rotor shaft may take a dynamic mode shape such that the displacement at the sensor location may not be the same as the magnetic bearing centerline displacement. The command signal is taken from the sensor location but the actuator applies the force through the coil such that the average force acts at the bearing centerline. This variation in command signal and actuator location is unique to the active magnetic bearings and may be used to the advantage of the designer to help place critical speeds. The performance of the AMB supported machinery may be more accurately predicted if proper account is taken for sensor location. This requires a modified, iterative solution strategy for current standard state-of-the-art computer codes for critical speeds, forced response, and stability. To initially evaluate the influence of the sensor placement, a modified extended Jeffcott rotor model will be developed with an assumed deformation to study the sensitivity of rotor bending modes and response to sensor location.

AMB EXTENDED JEFFCOTT MODEL

The original rotor model developed by H. H. Jeffcott consists of a single mass on a flexible shaft supported by rigid bearings. Kirk and Gunter (1972) modified this model to study the effect of support flexibility and damping on the synchronous response of the single mass flexible rotor. This paper extends the original Jeffcott model by assuming the existence of AMB supports. The extended model adds journal mass, bearing stiffness and damping at bearing locations, and assumes rigid bearing pedestals. The AMB extended Jeffcott model is shown in Figure 2.

To develop the extended Jeffcott model the disk mass plus the two center quarters of the shaft mass are lumped at midspan, M_2. The journal and shaft end quarter masses are lumped at bearing locations and modeled as $M_1/2$. The model is assumed to be symmetric; therefore, it can be simplified to a two-degree-of-freedom (2DOF) system as shown in Figure 3. An unbalance force is shown at M_2, and a constant magnitude excitation force is shown acting on M_1.

The equations of motion (EOM) for the 2DOF system are written as follows:

$$M_2\ddot{r}_2 = M_2\omega^2 a e^{i\omega t} - C_2(\dot{r}_2-\dot{r}_1) - K_2(r_2-r_1) \qquad [1]$$

$$M_1\ddot{r}_1 = F\phi e^{i\omega t} + C_2(\dot{r}_2-\dot{r}_1) + K_2(r_2-r_1) - C_1\dot{r}_s - K_1 r_s \qquad [2]$$

In equations [1] and [2] the deflections at M_1 and M_2 are defined as r_1 and r_2 respectively. The deflection at the AMB sensor location is defined as r_s. It is indicated by the EOM that the bearing forces are proportional to the sensor location deflection - not the bearing location deflection, as would be the case with conventional fluid-film or antifriction bearings.

The sensor location deflection is calculated after assuming mode shapes of a half-period of a sine wave. These mode shapes, modeling the first and third modes, are shown in Figure 4. Using Figure 4, the equation for the sensor location deflection is written as follows:

$$r_s = r_1 + (r_2 - r_1)\sin(\pi\alpha/2) \qquad [3]$$

where,

$$\alpha = z_s/(L/2). \qquad [4]$$

Equation [4] defines the value α as the ratio between the sensor offset and the shaft half-span.

After substitution of equation [3], equations [1] and [2] can be written in matrix form as follows:

$$\begin{bmatrix} M_1 & 0 \\ 0 & M_2 \end{bmatrix} \begin{bmatrix} \ddot{r}_1 \\ \ddot{r}_2 \end{bmatrix} + \begin{bmatrix} C_1 & 0 \\ 0 & C_2 \end{bmatrix} \begin{bmatrix} \dot{r}_1 \\ \dot{r}_2 \end{bmatrix} + \begin{bmatrix} K_1 & 0 \\ 0 & K_2 \end{bmatrix} \begin{bmatrix} r_1 \\ r_2 \end{bmatrix} = \begin{bmatrix} F\phi e^{i\omega t} \\ M_2\omega^2 a e^{i\omega t} \end{bmatrix} \qquad [5]$$

By assuming a solution of $r = Re^{i\omega t}$, the matrix equation [5] can be written in the following form:

$$\begin{bmatrix} K_{11} & K_{12} \\ K_{21} & K_{22} \end{bmatrix} \begin{bmatrix} R_1 \\ R_2 \end{bmatrix} = \begin{bmatrix} F\phi \\ M_2\omega^2 \end{bmatrix} \qquad [6]$$

where,

$K_{11} = (K_1(1-\beta) + K_2 - M_1\omega^2) + i\omega(C_2 + C_1(1-\beta))$

$K_{12} = (K_1\beta - K_2) + i\omega(C_1\beta - C_2)$

$K_{21} = -K_1 - i\omega C_2$

$K_{22} = (K_2 - M_2\omega^2) + i\omega C_2$

$\beta = \sin \pi\alpha/2.$

INFLUENCE OF SENSOR LOCATION ON UNDAMPED NATURAL FREQUENCY

The influence of sensor location on the critical speeds of the AMB rotor system is initially investigated by calculating the natural frequencies of the extended Jeffcott Model. The sensor location is varied inboard and outboard of the bearing centerline by as much as 20% of half-span.

Eliminating damping terms, C_1 and C_2, from equation [6]; and solving for the determinant of the resulting stiffness matrix, results in the following equation for the natural frequencies:

$$\omega^4 - (1 - \beta)\frac{K_1}{M_1} + \frac{(M_1+M_2)}{M_1 M_2} K_2\omega^2 + \frac{K_1 K_2}{M_1 M_2} = 0. \qquad [7]$$

Equation [7] can be written in the following non-dimens onal form:

$$\Omega^2 - \left(1 - \frac{K}{M}(1 + K(1 - \beta))\right)\Omega + \frac{K}{M} = 0 \qquad [8]$$

where,

$M = M_1/M_2$

$K = K_1/K_2$

$\Omega = \omega^2/(K_2/M_2)$

Results from Natural Frequency Analysis of AMB Extended Jeffcott Model

To show how sensor location influences the first and third natural frequencies of various geometries of the extended Jeffcott model, the solution of equation [8] was graphed for alpha values ranging from -2.0 to 2.0. This exemplifies sensor separations of 20% of half-span both inboard and outboard of the bearing centerline. The results are shown for mass ratios, M, of 1.0 (Figure 5), and 0.25 (Figure 6). The stiffness ratio, K, varies from 0.1 up to 10 in each analysis.

The results are similar for both mass ratios. The sensitivity to non-colocation of bearing and sensor is increased in two different situations. An increase in sensitivity occurs as stiffness ratios increase. This is attributed to the fact that when the bearing stiffness increases relative to the shaft stiffness there is more bending energy in the rotor. This causes a greater difference between bearing and sensor deflection at higher stiffness ratios. The sensitivity also increases as sensor-bearing separation increases. This also results in greater differences between bearing and sensor deflections.

The direction in which the criticals move depends on whether the sensor, at an inboard or outboard location, gives more or less response than the normal bearing centerline. For the first mode, the inboard sensors have a greater deflection than the bearings; therefore, the critical increases due to higher bearing forces. Outboard sensors detect less deflection than at the bearing, thus decreasing bearing forces and lowering the critical frequency. The opposite occurs at the third mode. The inboard sensors detect less deflection, while the outboard sensors detect more deflection than at the bearing centerline. This lowers the third critical frequency for inboard sensors and raises it for outboard sensors.

INFLUENCE OF SENSOR LOCATION ON FORCED RESPONSE SOLUTION

The response is calculated for two forms of excitation applied independently to the AMB extended Jeffcott model equations. In order to calculate the response, the matrix equation [6] is solved for R_1 and R_2 using Cramer's Rule (Anton, 1984). The solution has the following form:

$$R_1 = \frac{F\phi\ K_{22} - K_{12}(\ M_2 a\omega^2\ )}{K_{11}\ K_{22} - K_{12}\ K_{21}} \qquad [9]$$

$$R_2 = \frac{K_{11}(\ M_2 a\omega^2\ ) - F\phi\ K_{21}}{K_{11}\ K_{22} - K_{12}\ K_{21}} \qquad [10]$$

The resulting response is complex, thus there exists an amplitude and a phase angle associated with both R_1 and R_2. The phase angles can be obtained from the following equations:

$$\theta_1 = \cos^{-1}\left[\frac{\text{real}(R_1)}{\text{sqrt}[\{\text{real}(R_1)\}^2 + \{\text{imag}(R_1)\}^2]}\right] \qquad [11]$$

$$\theta_2 = \cos^{-1}\left[\frac{\text{real}(R_2)}{\text{sqrt}[\{\text{real}(R_2)\}^2 + \{\text{imag}(R_2)\}^2]}\right] \qquad [12]$$

It must be noted at this point that the unbalance force and the constant excitation force are never applied at the same time as this introduces additional complexities not accounted for by the Jeffcott model. Physically, the constant magnitude excitation force is applied in one plane only, therefore the motion of the masses is in one plane only. However, for computational and analytical simplicity, it will be assumed that the constant magnitude excitation force acts in two mutually perpendicular planes in a manner similar to the unbalance force. The correct solution for the constant magnitude excitation force plane, is then, simply the real part of the deflections R_1 and R_2 shown above. However, since the motion is assumed to be circular, the maximum amplitudes in the X-direction, X_1 and X_2, will be the same as R_1 and R_2, for masses M_1 and M_2. Similarly, the phase angles calculated from R_1 and R_2 are also valid for motion in one plane. Thus, regardless of whether an unbalance force or a constant magnitude excitation force is applied, the solution technique and the solution itself will remain the same.

Results from Forced Response Analysis of AMB Extended Jeffcott Model

The results that are to be shown are of the bearing journal response. Similar results occur for the mid-span mass response; therefore, they are omitted.

The response amplitude at the bearing location is plotted versus shaft frequency in Figure 7. The excitation causing this response is due to an imbalance at mid-span resulting from an eccentricity of 0.076 mm at M_2. In this case M = 1.0, K = 2.0, and the bearing damping is set to 0.283 N-s/mm. The shaft damping is assumed negligible. The value of α, being varied as in the critical speed solution, ranges from -0.2 to 0.2.

In Figure 7 it can be seen that the first mode peak resonance frequencies increase from the colocation case, $\alpha = 0$, when inboard sensors, $\alpha > 0$, are used. The peak frequencies are shown to decrease with outboard sensor, $\alpha < 0$, use. For the third mode, the peak frequencies are lower with inboard sensor use, and raised for outboard sensor use. These results are very consistent with the results shown from the influence of sensor location on natural frequencies. The same reasoning can be used to explain both sets of results.

The results from the case using a constant magnitude excitation at the bearing location shows the same tendencies as the unbalance case. Shown in Figure 8 are the results of the bearing location excitation case.

CONCLUSIONS

This preliminary investigation into the effect of sensor location on the rotor dynamic performance of AMB turbomachinery gives very useful results. The natural frequency and forced response results from the AMB extended Jeffcott model could give the rotor-bearing system designer greater confidence in the proper selection of sensor location.

From the test run of the AMB extended Jeffcott model the following specific conclusions were made:

1. For inboard sensors, as the sensor is moved away from the bearing, the first mode critical frequency goes higher. For outboard sensors, as the sensor is moved away from the bearing, the first mode critical frequency goes lower.

2. For inboard sensors, as the sensor is moved away from the bearing the third mode critical frequency decreases. However for outboard sensors, as the sensor is moved away from the

bearing the third mode critical frequency increases.

3. The vibrational characteristics of the two mass rotor system did not vary when a constant excitation force was used instead of a rotating unbalance.

4. The effect of the sensor position on the critical frequencies was considerable, when the stiffness ratio was high.

5. Higher mass ratios led to increased sensitivity of third mode critical frequency to changing sensor positions. Vice versa, low mass rations led to increased damping effects in the third mode, making the rotor relatively insensitive to changing sensor locations.

RECOMMENDATIONS

The AMB extended Jeffcott model is a simple but very useful approximation of a much more complex rotor-bearing system. The following recommendations are made for extending the current approximate analysis:

1. The addition of pedestal stiffness and damping should be included in this model.

2. A method for accounting for sensor location should be included in the transfer matrix codes that are used to calculate forced response.

3. This research should be extended to a stability analysis in order to improve prediction capability for AMB turbomachinery.

4. Experimental test results must be generated for comparison and verification of the analyses developed.

REFERENCES

Hustak, J. F., R. G. Kirk, and K. A. Schoeneck, 1987, "Analysis and Test Results of Turbocompressors Using Active Magnetic Bearings," Lubrication Engineering, Vol. 43, No. 5, pp. 356-362.

Kirk, R. G., J. F. Hustak and K. A. Schoeneck, 1988, "Analysis and Test Results of Two Centrifugal Compressors Using Active Magnetic Bearings," Vibrations in Rotating Machinery, I. Mech. E. Proceedings of 4th International Conference, Edinburg, pp. 93-100.

Kirk, R. G., and E. J. Gunter, Jr., 1972, "The Effect of Support Flexibility and Damping on the Synchronous Response of a Single-Mass Flexible Rotor," ASME Trans., J. of Engrg. for Industry, Vol. 94, Series B, No. 1.

Myklestad, N. O., 1944, "A New Method of Calculating Natural Modes of Uncoupled Bending Vibration of Airplane Wings and Other Types of Beams," J. of Aeronautical Sciences, pp. 153-162.

Prohl, M. A., 1945, "A General Method for Calculating Critical Speeds of Flexible Rotors," J. of Applied Mechanics, pp. 142-148.

Schoeneck, K. A., and J. F. Hustak, 1987, "Comparison of Analytical and Field Experience for a Centrifugal Compressor Using Active Magnetic Bearings," I. Mech. E. Conference Proceedings, The Hague, Netherlands, May 18-20.

ACKNOWLEDGMENT

This work has been sponsored by a joint industry/Virginia Center for Innovative Technology Research Grant No. CAE-89-015, with matching funds from Dresser-Rand Co. and Magnetic Bearings, Inc. The authors are especially grateful for the support given by Dr. Ira Jacobson, Director of the Institute of Computer Aided Engineering, Charlottesville, Virginia.

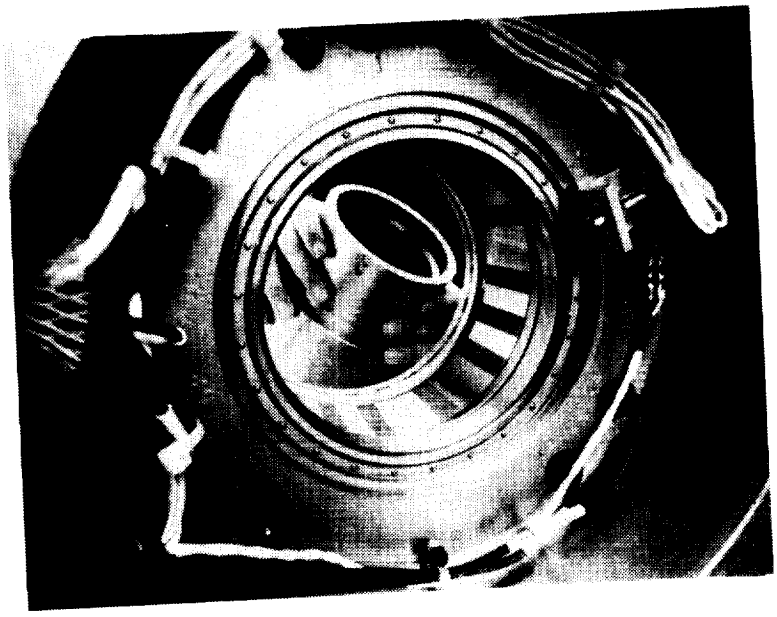

Figure 1. Picture of active magnetic bearing

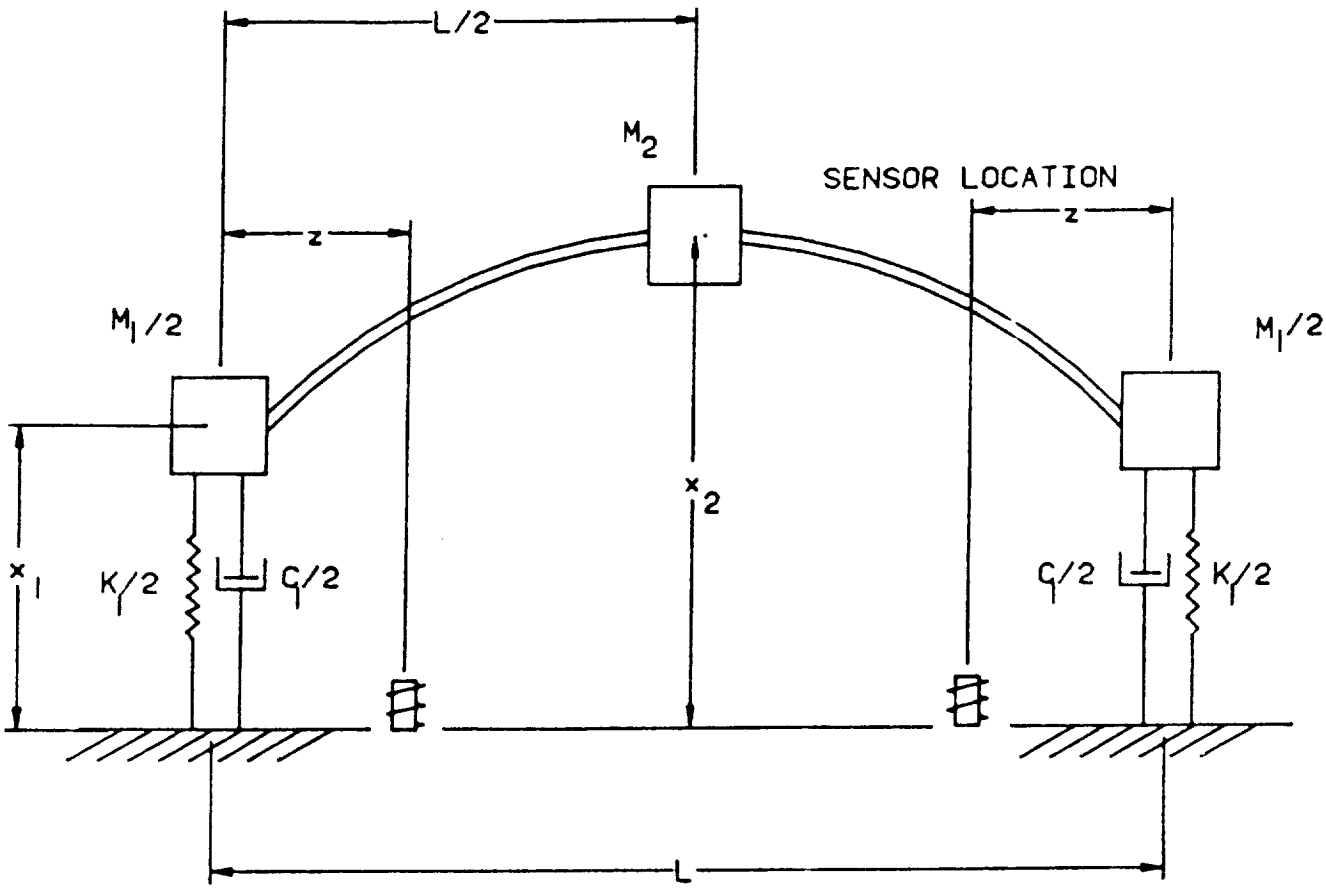

Figure 2. The modified Jeffcott model

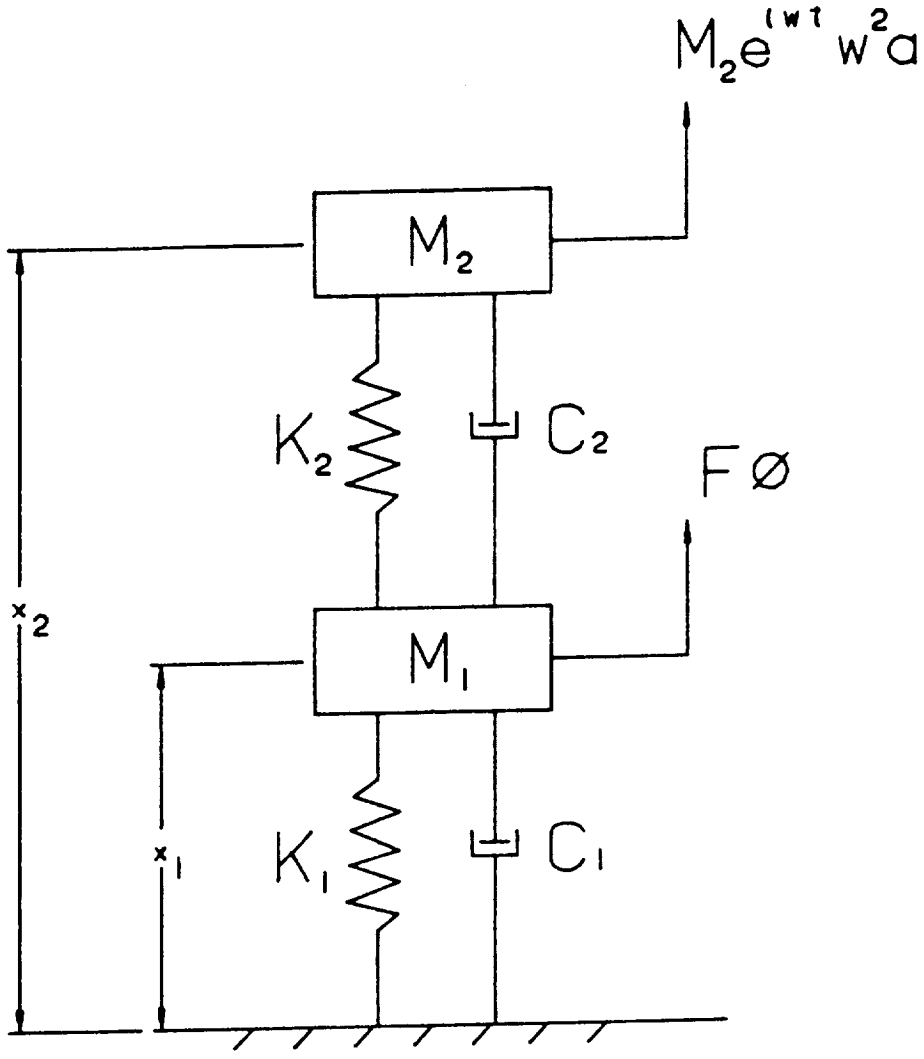

Figure 3. Reduced two DOF representation of the modified Jeffcott model

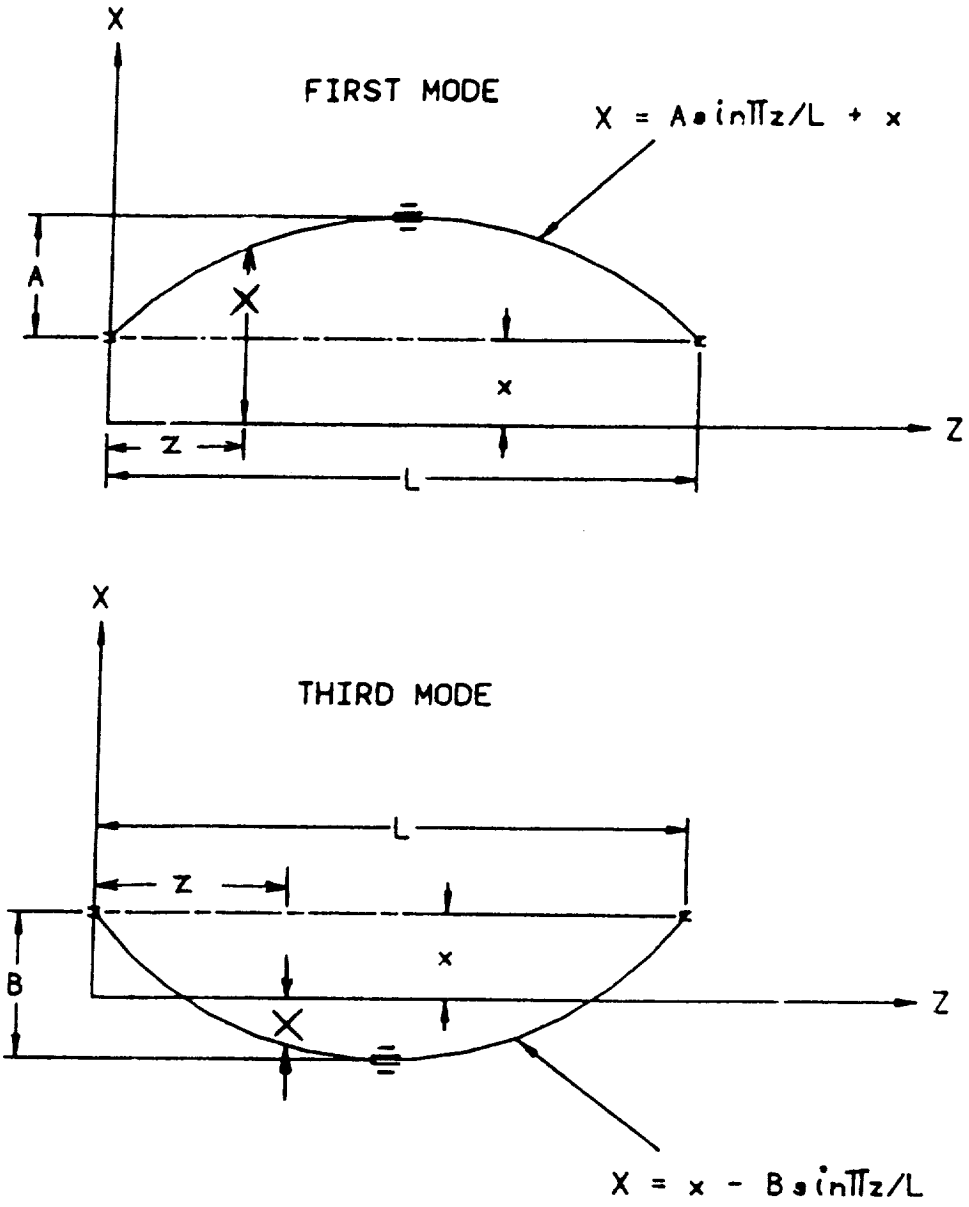

Figure 4. Mode shapes for the modified Jeffcott model

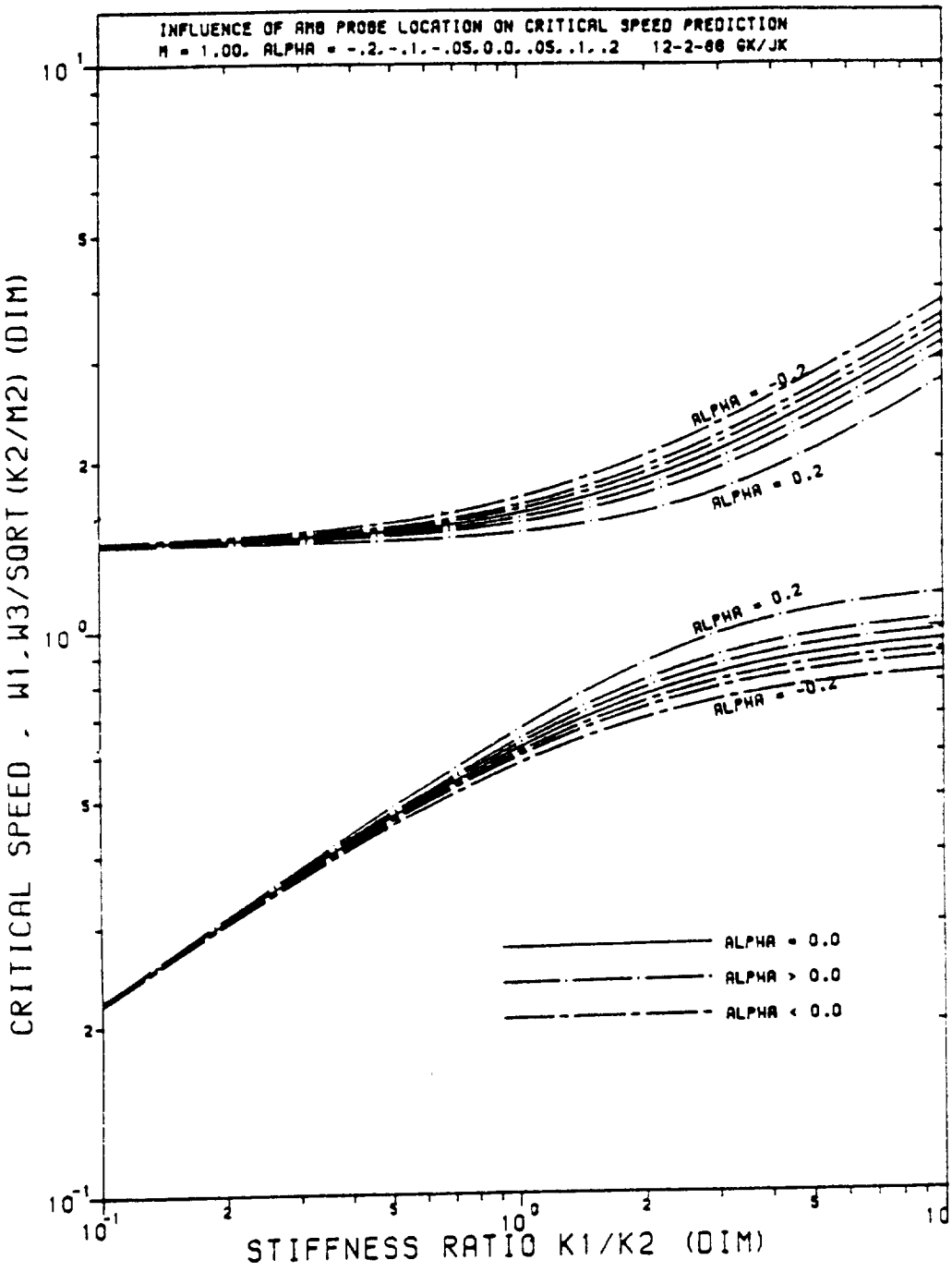

Figure 5. Critical speed map for M = 1.0 from AMB modified Jeffcott analysis

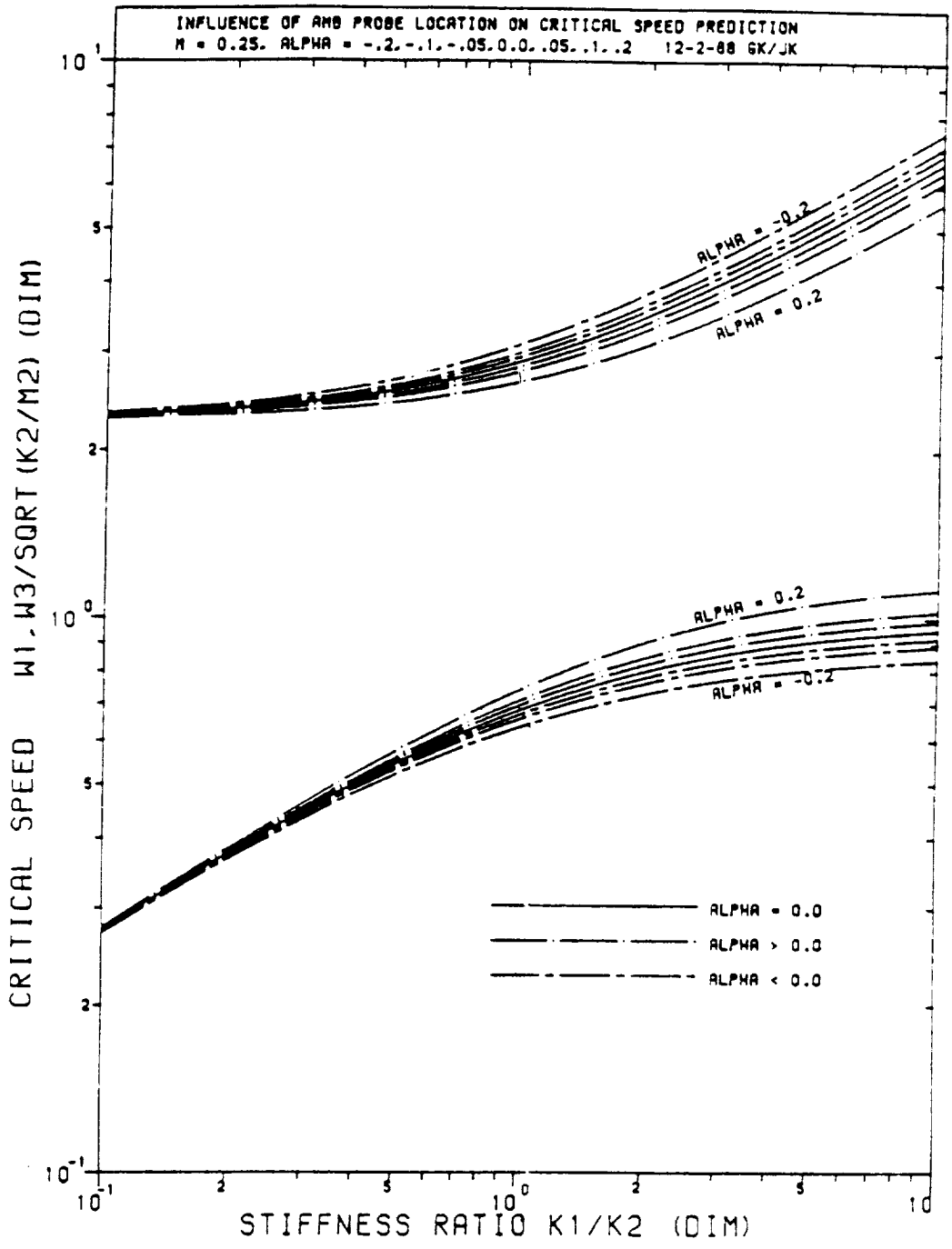

Figure 6. Critical speed map for M = 0.25 from AMB modified Jeffcott analysis

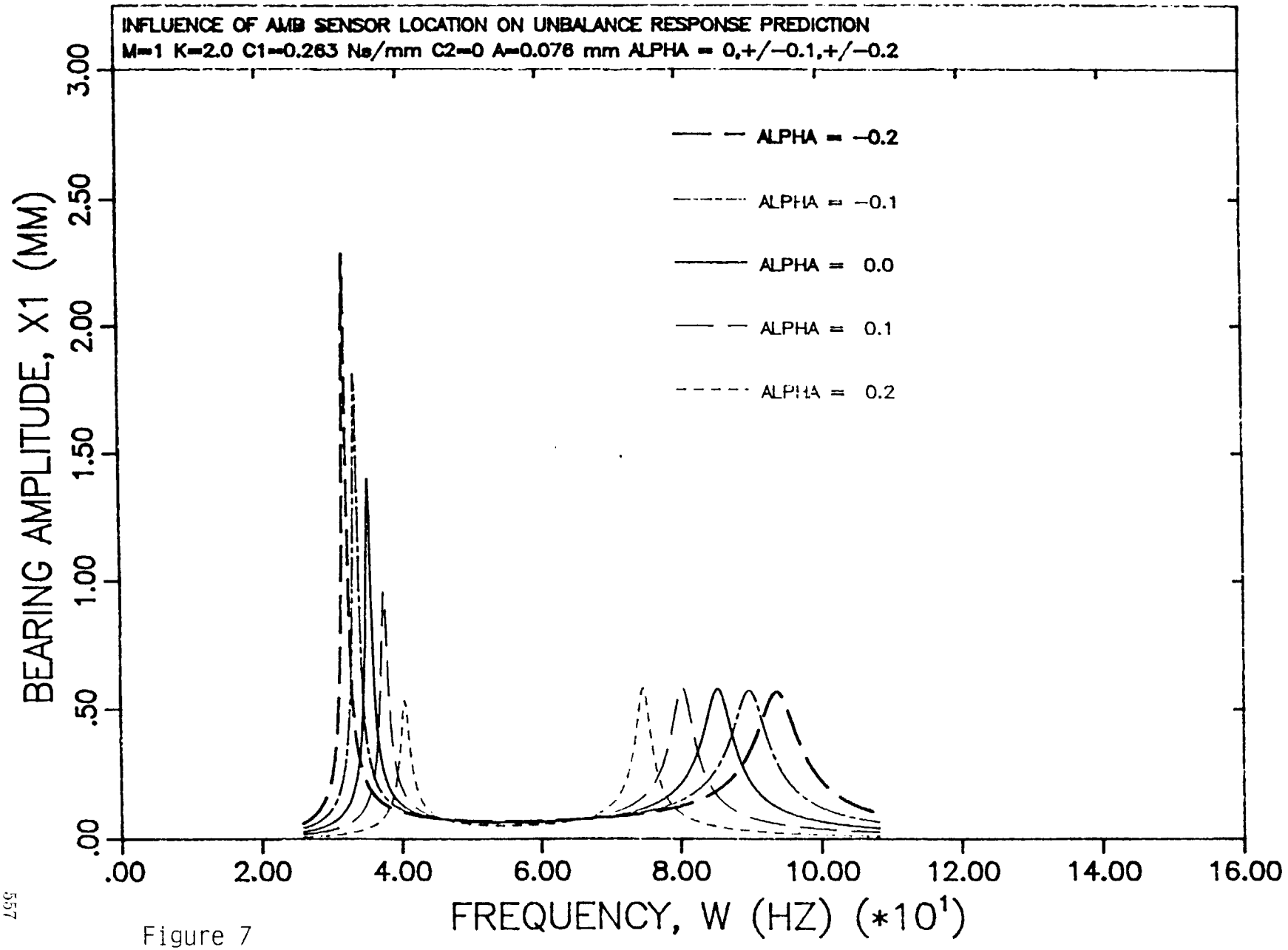
INFLUENCE OF AMB SENSOR LOCATION ON UNBALANCE RESPONSE PREDICTION
M=1 K=2.0 C1=0.263 Ns/mm C2=0 A=0.076 mm ALPHA = 0,+/-0.1,+/-0.2
ALPHA = -0.2
ALPHA = -0.1
ALPHA = 0.0
ALPHA = 0.1
ALPHA = 0.2
BEARING AMPLITUDE, X1 (MM)
.00
.50
1.00
1.50
2.00
2.50
3.00
.00
2.00
4.00
6.00
8.00
10.00
12.00
14.00
16.00
FREQUENCY, W (HZ) (*10¹)

Figure 7

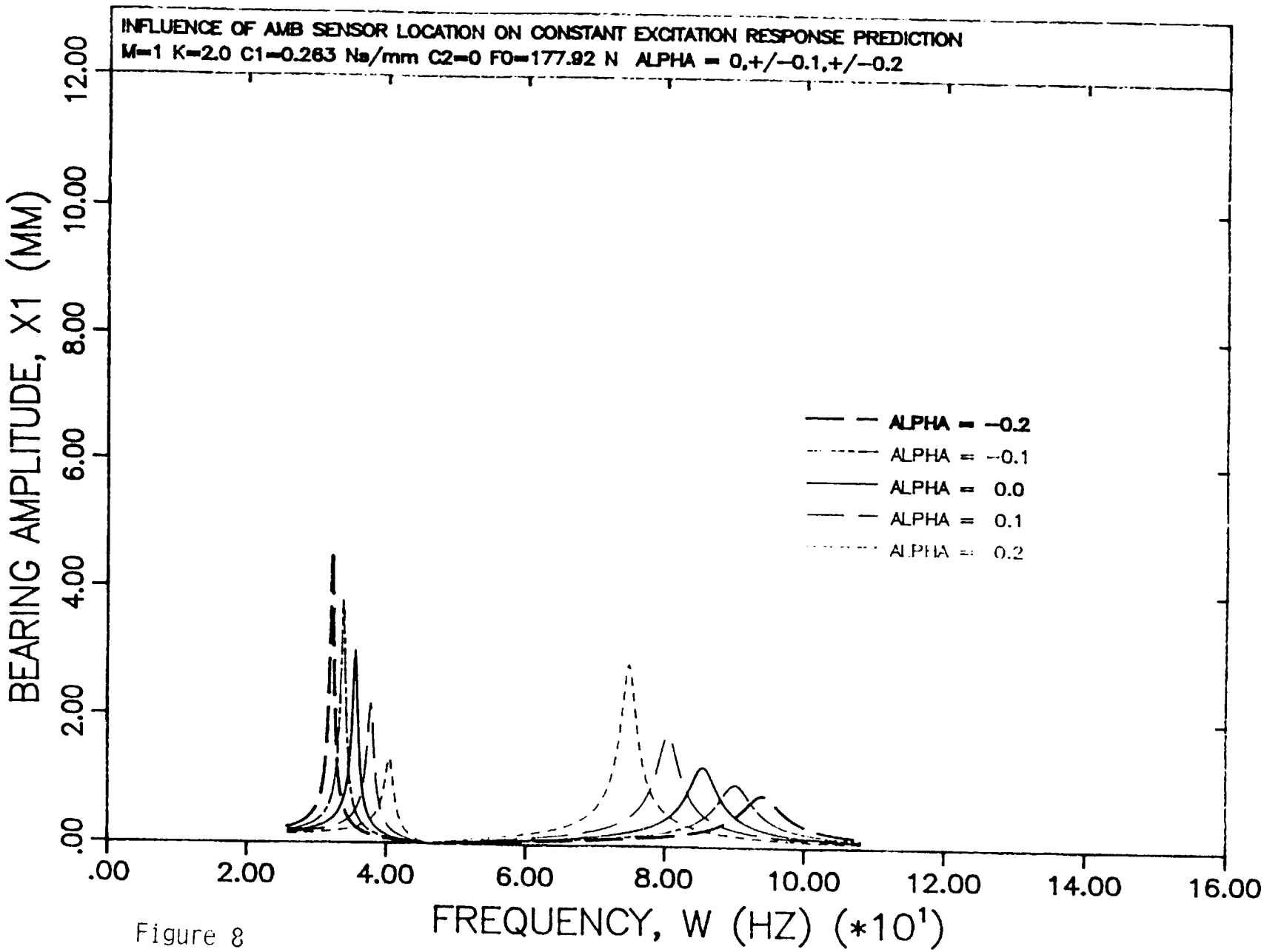
INFLUENCE OF AMB SENSOR LOCATION ON CONSTANT EXCITATION RESPONSE PREDICTION
M=1 K=2.0 C1=0.263 Ns/mm C2=0 F0=177.92 N ALPHA = 0,+/-0.1,+/-0.2
BEARING AMPLITUDE, X1 (MM)
.00
2.00
4.00
6.00
8.00
10.00
12.00
FREQUENCY, W (HZ) (*10¹)
14.00
16.00
ALPHA = -0.2
ALPHA = -0.1
ALPHA = 0.0
ALPHA = 0.1
ALPHA = 0.2

Figure 8